TOWARDS AN INDUSTRIAL LASER DOPING PROCESS FOR THE SELECTIVE EMITTER USING PHOSPHORIC ACID AS DOPANT

M. Eberstein[1], M. Geier[1], H. Grießmann[1], U. Partsch[1], L. Voelkel[2,a], R. Böhme[2,b], S. Pentzien[3], R. Koter[3], G. Mann[3], J. Bonse[3], J. Krüger[3]

[1] Fraunhofer IKTS, Winterbergstr. 28, 01277 Dresden, Germany
[2] Roth & Rau AG, An der Baumschule 6-8, 09337 Hohenstein-Ernstthal, Germany
[3] BAM Bundesanstalt für Materialforschung und –prüfung, Unter den Eichen 87, 12205 Berlin, Germany
[a] now with Globalfoundries, [b] now with InnoLas Systems GmbH

ABSTRACT: Different laser supported approaches have already been realized, proving the great potential of laser-doped selective emitters (LDSE). However, it is challenging to establish a low-cost process by using pulsed laser tools. So far a single-step process only leads to satisfying results utilizing cw-lasers. In this paper we have examined a two-step process to produce laser-doped selective emitters on multicrystalline textured standard silicon photovoltaic wafers (90-Ω/sq-Emitter, SiN-antireflection coating (ARC)). The precise ARC removal by near-infrared fs-laser pulses (30 fs, 800 nm), and the doping of uncoated silicon wafers by ns-laser pulses (8 ns, 532 nm) were systematically investigated. In the fs-experiment, optimum conditions for ARC removal were identified. In the ns-experiments under suitable conditions (melting regime), the phosphorous concentration underneath the wafer surface was significantly increased and the sheet resistance was reduced by nearly a factor of two. Moreover, electrical measurements on fired metallization fingers deposited on the laser processed wafers showed low contact resistances. Hence, wafer conditioning with combined fs-laser- and ns-laser-processes are expected to be a promising technology for producing selective emitters.

Keywords: Laser Processing, Doping, Selective Emitter, Multicrystalline Silicon

1 INTRODUCTION

The selective emitter (SE) consists of a tailored, emitter doped area with typical doping concentrations of at least 10^{20} phosphorous atoms per cm^3 under the front-side contact finger of a solar cell, resulting in a reduced electrical resistance in that area. The doping in the non-metallized cell area can, therefore, be less than in a standard cell (e.g. 120-Ω/sq instead of 60-Ω/sq) resulting in higher yield of light in the crystalline Si and in reduced recombination losses at the cell surface. Different technological approaches including laser processes have already been realized [1-3], proving the great potential of laser-doped SEs (LDSE) typically leading to an increase of the overall efficiency between 0.5% and 1%. However, it is challenging to establish a low-cost process which can be used in an industrial production line environment.

Coating the silicon-based PV-wafer with phosphoric acid as dopant source and the subsequent use of a laser beam for opening the anti-reflection coating (ARC, typically made of silicon nitride) while simultaneously doping the underlying region (silicon) is one promising concept for the production of SEs [4]. Simultaneous opening and doping on the laboratory scale using a cw-laser was reported [5]. In this paper we have split the laser-doping in a two-step laser process, systematically investigating the precise ARC removal by near-infrared fs-laser pulses (30 fs, 800 nm), and the doping of uncoated silicon wafers by ns-laser pulses (8 ns, 532 nm). Limiting effects of the laser pulse - material interaction are identified, process windows are examined and suggestions for successful realization of LDSE are given.

2 EXPERIMENTAL

Our investigations on a laboratory scale examine laser based opening of the ARC on multi-crystalline industrial standard photovoltaic wafers (textured polycrystalline silicon, 90-Ω/sq-Emitter, with SiN-antireflection coating). A commercial fs-laser amplifier system (Femtopower Compact Pro, Femtolasers) was used, which emits ultrashort laser pulses (~30 fs duration, max. repetition rate 1 kHz) at a central wavelength of 800 nm. These pulses were focused in air to the sample surface by means of a concave mirror. The $1/e^2$-diameter of the focus was between 200 µm and 300 µm. Laser fluences (peak value in front of the sample) and modification thresholds were determined using a technique described in [6] for dielectric layers which is applicable for thin film photovoltaic materials, too [7]. The fs-laser irradiation results were inspected by optical microscopy using differential interference contrast mode (DIC). Selected irradiated areas were subjected to scanning electron microscopy (SEM).

For the formation of a selective doped silicon area a commercial diode-pumped ns-laser system (DiNY pQ, IB Laser), which emits laser pulses (8 ns pulse duration, max. repetition rate 0.5 kHz) at a wavelength of 532 nm, was utilized. These pulses were focused in air to the sample surface with the help of a galvano scanner equipped with an F-theta optic. The $1/e^2$-diameter of the focus was ~200 µm. The ns-laser irradiation results were inspected by digital microscopy. The samples for the ns-laser doping experiments were standard wafers (textured polycrystalline silicon, 120-Ω/sq-Emitter, with SiN-antireflection coating). Prior to ns-laser processing, the SiN-layer was removed (stripped) by chemical etching. These stripped wafers were coated by phosphoric acid (H_3PO_4) and dried subsequently. After the laser irradiation experiments the wafers were characterized by depth-profiling secondary ion mass spectrometry (SIMS, Cameca ims4fE6:Cs^+) tracking the phosphorous atomic concentration as a function of the sputter depth in an area of 30×30 µm^2. Additionally, electrical parameters of the subsequently metalized wafers later used for the solar cells were acquired (home-built measuring setup of the IKTS).

3 RESULTS

3.1 Fs-laser-based opening of the ARC-layer

First, the ablation threshold of the SiN-layer was determined with varying laser pulse energies between 54 µJ and 400 µJ. The corresponding peak energy densities can be obtained by multiplying by a factor of 3.2×10^{-3} J cm^{-2}/µJ. The ablation threshold of the SiN-layer was found at about 35 µJ (0.11 J cm^{-2}). By the (partial) removal of the SiN-layer, its anti-reflection effect is reduced. The ablated areas therefore appear bright.

With selected laser pulse energies line structures with different degrees of pulse-overlapping (effective number of pulses per ablation-diameter, N_{eff}) were generated by linear movement of the sample across the fs-laser beam.

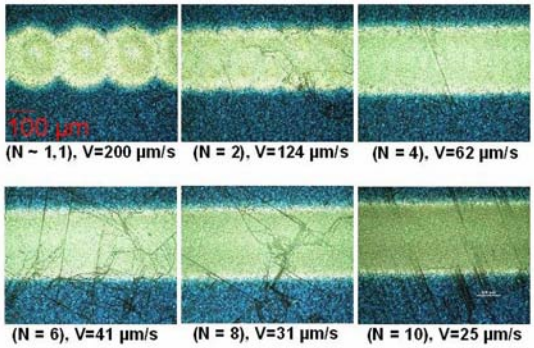

Figure 1: Optical micrographs of fs-laser ablated lines in the SiN-layer of a standard PV-wafer using a pulse energy of E = 238 µJ and different scan velocities between 25 µm/s and 200 µm/s.

Figure 1 shows an example of such an ablation-line with a pulse energy of E = 238 µJ, which was created with a laser pulse repetition rate of 1 Hz and sample translation rates between 25 µm/s and 200 µm/s. The corresponding effective number of pulses ranged from N_{eff} ~ 1.1 (v = 200 µm/s, low spot-overlap) and N_{eff} = 10 (v = 25 µm/s, large spot-overlap). For N_{eff} ~ 1.1, the ablation effects of individual spots can be identified. With increasing N_{eff}, the ablated line structures slightly widen and the ablated structures appear somewhat darker.

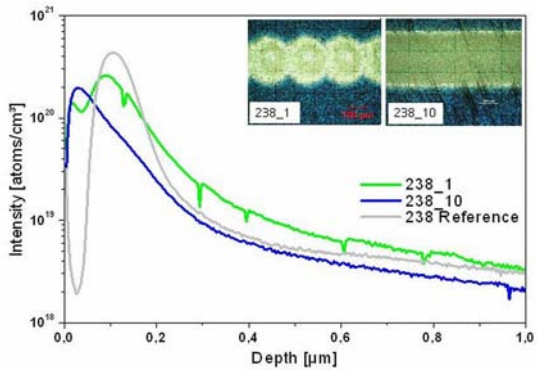

Figure 2: Depth profiles (SIMS) of the near surface phosphorous concentration in the center of fs-laser ablated line structures (E = 238 µJ) with two different pulse overlaps [N_{eff} ~ 1.1 (green) and 10 (blue)]. For comparison a reference spectrum in the non-irradiated area is shown (gray). The inserts show optical micrographs of both line structures.

In addition, cracks can be seen on the sample material (N_{eff} = 2, 4, 6, 8) that were not created by laser irradiation, but were already present inside the sample material prior to the irradiation. For N_{eff} = 10, there are scratches on the coated silicon surface that diminish via the fs-laser-induced ablation of the SiN-layer and a part of the underlying silicon.

Figure 2 shows phosphorous depth profiles (SIMS) from ablated lines that were generated with a laser pulse energy of 238 µJ and varying effective number of pulses (N_{eff} ~ 1.1: green curve and N_{eff} = 10: blue curve). A reference spectrum of the non-irradiated surface is shown for comparison. The partial ablation of the SiN-layer shifts the maximum of the phosphorous concentration towards the surface (to smaller depths).For the small pulse-overlap (N_{eff} ~ 1.1), the phosphorous concentration is higher than 10^{20} cm^{-3} up to a depth of ~0.2 µm. For the larger pulse-overlap (N_{eff} = 10), the phosphorous concentration is already significantly reduced due to material ablation (manifesting in a horizontal shift of the blue curve compared to the green one).

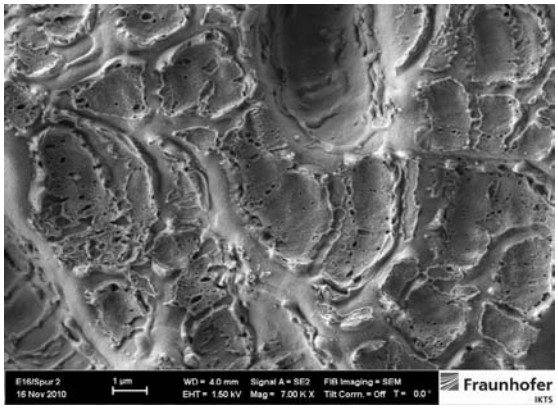

Figure 3: SEM image of a surface area in the central part of a fs-laser ablated line on a standard silicon PV-wafer (E = 85 µJ, N_{eff} ~ 1.1).

Figure 3 shows a SEM image of the wafer surface in the center of a fs-laser ablated line using E = 85 µJ pulse energy and a pulse overlap of N_{eff} ~ 1.1. It can be seen, that the protruding edges of the textured surface material were ablated while in the valleys SiN-layer relicts were left behind. Hence, an optimum between laser pulse energy and pulse overlap has to be found where the SiN-layer is already open and the emitter layer is not ablated significantly. Opening the SiN-layer by single laser pulses with 238 µJ (0.75 J cm^{-2}) pulse energy, the emitter remains largely preserved as already seen in Fig. 2 (green curve). Consequently, a pulse energy of 238 µJ and a small pulse-overlap (N_{eff} ~ 1.1) are promising parameters for a subsequent ns-laser doping process, followed by metallic paste contacting.

3.2 Ns-laser-based doping of multicrystalline silicon wafers

In a first step, the H_3PO_4-layer was washed with water in an ultrasonic bath to obtain a bare Si wafer. Laser modification thresholds were tested on this bare

(without ARC coating and without phosphoric acid) silicon wafer surface to avoid any confusion with the "laser cleaning" threshold of H_3PO_4. From these experiments, the relevant energy level could be estimated. About 50 µJ pulse energy was needed to modify the surface of the silicon wafer permanently. In a second step, ns-laser irradiated fields with a size of 2 ×2 mm² were scanned on the surface of the H_3PO_4 coated wafers (without ARC coating) with eight different laser pulse energies (50 µJ – 1000 µJ) and with six different linear pulse overlap degrees (N_{eff} = 1, 2, 4, 6, 8, 10). In the ns-case, the corresponding peak fluences can be calculated from the laser pulse energies by multiplication with the factor of 6.4×10^{-3} J cm^{-2}/µJ.

Figure 4 shows a digitally recorded optical micrograph (overview) of the laser-treated Si-PV-wafer. In selected 2 × 2 mm² fields, depth profiles of the phosphorous concentration were recorded using SIMS.

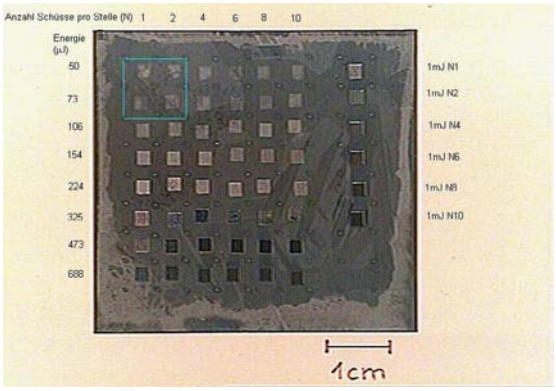

Figure 4: Digitally recorded optical micrograph (overview) of a phosphoric acid coated Si-PV-wafer (without SiN) modified by ns-laser irradiation with different laser pulse energies (rows) and effective pulse numbers per spot (columns).

Figure 5 shows a compilation of phosphorus-depth profiles from fields that were irradiated with three different pulse energies (E = 50 µJ, 224 µJ and 668 µJ) and varying pulse-overlap (N_{eff} = 1 or 10).

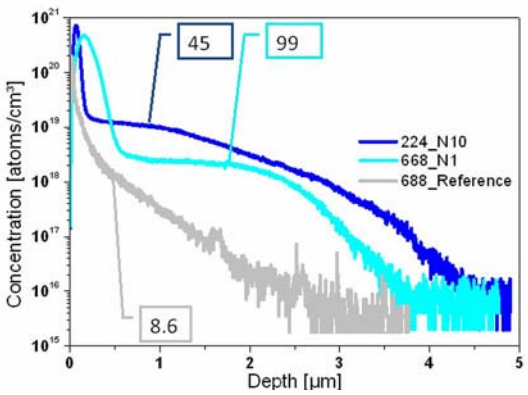

Figure 5: Phosphorous depth-profiles (SIMS) in selected ns-laser-modified fields of H_3PO_4-coated Si-PV-wafers.

The ns-laser process leads to an accumulation of phosphorus in the surface-near zones (up to 5 µm below the surface), which could be determined by comparing the integrals of the profile curves. The highest energy in the melting regime (E = 224 µJ, N_{eff} = 10) showed a significant recovery of phosphorus (integral: 45 [a.u.] (see the blue curve) compared to 8.6 [a.u.] (gray curve) for the reference position). Irradiation at high energies (ablation regime) with low pulse overlap also showed a large integrated phosphorus concentration (integral: 99 [a.u.] (cyan curve)). These conditions, i.e., moderate effective pulse numbers (N_{eff}~10) in the melting regime or N_{eff} ~1 for fluences slightly above the ablation threshold, are promising candidates for a successful ns-laser-based doping process.

After successful production of structures (2 × 2 mm² fields) suitable for the measurement of electric properties, the sheet and the contact resistance were characterized within the laser-irradiated areas via two- or four-point-measurements. Figure 6 shows the sheet resistance (4-point measurement) as a function of the laser pulse energy for constant pulse overlap (N_{eff} = 4). While no clear correlation of sheet resistance with the pulse energy in the ablation-regime ($E \geq$ 473 µJ) can be observed, a reduction from the reference value of the non-irradiated wafer material (120-Ω/sq) to a value around 90-Ω/sq can be seen in the melting regime (106 µJ - 224 µJ). This indicates that phosphorous was successfully incorporated into the silicon host material and should, therefore, be usable for the selective emitter.

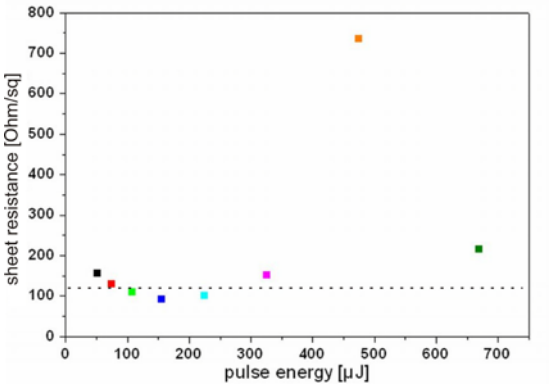

Figure 6: Results of sheet resistance measurements within the ns-laser-doped measuring structures upon variation of the laser pulse energy (at fixed effective pulse number per spot, N_{eff} = 4).

To investigate the contact formation using a thick film paste, the wafers were subsequently metallized using aerosol printing (Heraeus DSP109-054, parallel lines with 1.3 mm length, 38 µm width, and 0.39 mm distance) and firing in standard conditions for solar cells. The firing temperature was varied in 20 K steps between 840 °C and 920 °C. The measuring setup used and the results of electrical contact resistance measurements are summarized in Figure 7. In the ns-laser-induced melting regime (E = 150 µJ and 224 µJ), as expected, the contact resistance is reduced to values as low as 5 mΩ cm^2 (224 µJ, N_{eff} = 1). This meets the paste manufacturers specification for a 60-Ω/sq standard wafer. In the ablation regime (E = 668 µJ) the contact resistance rises significantly. Here, the formation of a surface passivation-layer could be detected using SEM. By comparing the curves 224 µJ, N_{eff} = 1 and 224 µJ, N_{eff} = 2 it can be seen, that larger spot overlap also leads to higher contact resistances.

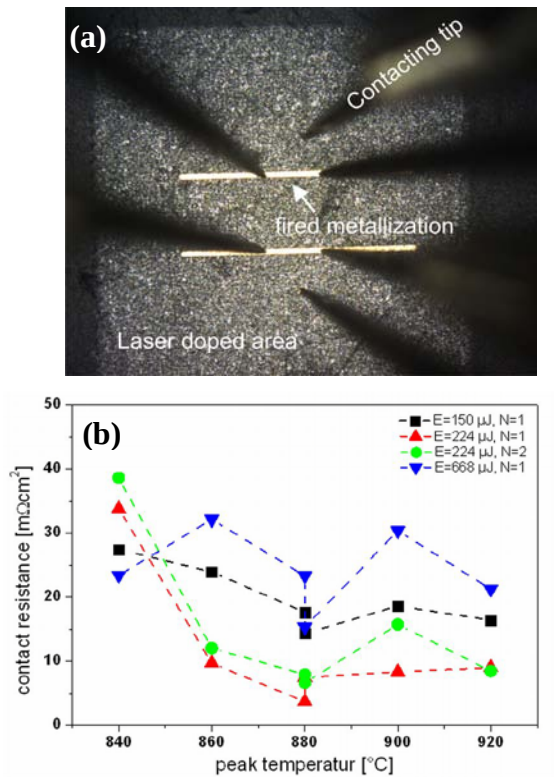

Figure 7: (a) Optical micrograph of the electrical resistance measurement setup; the two bright horizontal lines represent the metallic contacts (b) Contact resistance as a function of the firing temperature for laser-doping at small pulse overlaps (N_{eff}~1-2). The lines guide the eye.

4 SUMMARY

A two-step process to produce laser-doped selective emitters (LDSE) on multicrystalline textured standard silicon wafers (90-Ω/sq-Emitter, SiN-antireflection coating) was examined. The precise ARC removal by near-infrared fs-laser pulses (30 fs, 800 nm), and the doping of uncoated silicon wafers by ns-laser pulses (8 ns, 532 nm) were systematically investigated. In the fs-experiments an optimum where the SiN-layer (ARC) is opened to a large extent but the underlying original emitter-layer is not ablated significantly was identified (E = 238 µJ [0.75 J cm^{-2}], N_{eff} = 1.1 – 2).

In ns-laser doping experiments, a melting or ablation regime can be observed for stripped silicon PV-wafers using dried phosphoric acid as dopant. Indications for the formation of a surface passivation-layer were found in the ablation regime for large pulse overlap. In the melting regime, the phosphorous concentration underneath the wafer surface was significantly increased and the sheet resistance dropped by ~25%. Moreover, electrical measurements on fired metallization fingers deposited on the laser processed wafers showed promising contact resistances as low as 5 mΩ cm^2 only. This meets the paste manufacturers specification for a 60-Ω/sq standard wafer.

Hence, wafer conditioning with combined fs-laser- and ns-laser-processes is expected to be feasible for producing selective emitters.

ACKNOWLEDGEMENT: The authors would like to thank M. Ihle and S. Hildebrandt (both at the Fraunhofer IKTS) for the aerosol printing of the metallization lines.

5 REFERENCES

[1] K.S. Wang, B.S. Tjahjono, J. Wong, A. Uddin, S.R. Wenham, Solar Energy Materials & Solar Cells 95 (2011) 974.
[2] M. Bähr, G. Heinrich, K.-P. Stolberg, T. Wütherich, R. Böhme, Proceedings of the 25th PVSEC, Valencia (2010) 2490.
[3] F. Colville, Photovoltaics International 3rd Edition, (2009) PVI5-01_3.
[4] J.R. Köhler, P. Grabitz, S.J. Eisele, T.C. Röder, J.H. Werner, 24th PVSEC, Hamburg (2009) 1847.
[5] A. Sugianto, J. Bovatsek, S. Wenham, B. Tjahjono, X. Guangqi, Y. Yu, B. Hallam, B. Xue, N. Kuepper, C. M. Chong, R. Patel, Proceedings of the 35th IEEE Photovoltaic Specialists Conference (2010) 689.
[6] J. Bonse, S. Baudach, W. Kautek, E. Welsch, J. Krüger, Thin Solid Films 408 (2002) 297.
[7] J. Bovatsek, A. Tamhankar, R.S. Patel, N.M. Bulgakova, J. Bonse, Thin Solid Films 518 (2010) 2897.